Acoustic and mechanical testing of commercial cocoa powders

Lubomír Lapčík, Barbora Lapčíkova, Shweta Gautam, Martin Vašina, Tomáš Valenta, David Řepka, Klára Čépe & Ondřej Rudolf

View supplementary material ☐

Published online: 29 Sep 2022.

Submit your article to this journal ☐

Article views: 279

View related articles ☐

View Crossmark data ☐

Taylor & Francis
Taylor & Francis Group

Acoustic and mechanical testing of commercial cocoa powders

Lubomír Lapčík [a,b], Barbora Lapčíková [a,b], Shweta Gautam [b], Martin Vašina [b,c], Tomáš Valenta [b], David Řepka [a], Klára Čépe [d], and Ondřej Rudolf [b]

aDepartment of Physical Chemistry, Faculty of Science, Palacky University Olomouc, Olomouc, Czech Republic; bFaculty of Technology, Tomas Bata University in Zlín, Zlin, Czech Republic; cDepartment of Hydromechanics and Hydraulic Equipment, Faculty of Mechanical Engineering, VSB-Technical University of Ostrava, Ostrava-Poruba, Czech Republic; dCATRIN – Regional Centre of Advanced Technologies and Materials, Palacky University Olomouc, Olomouc, Czech Republic

ABSTRACT

In the present study, commercial cocoa powders with different cocoa fat contents were studied. It was found that the cocoa powders' flow patterns were of a cohesive to highly cohesive characters. It was demonstrated, that the powders of higher crystalline structure were less flowable compared to the ones with the more amorphous ones. It was observed by SEM that the studied cocoa powders of higher cocoa fat content and the ones with the dietary fibers content (sample 2) exhibited more amorphous structure. The predominantly smooth surface structure of the higher fat content cocoa powder allowed its higher dense packing, triggering the decreased sound absorption typical for non-porous materials as quantified by NRC of 0.289 (sample 1, 100 mm material height) and 0.227 (sample 3) to 0.182 (sample 2). The latter conclusions were also supported by the observed increase of the structural mechanical stiffness of the freely poured powder bed of high cocoa fat amorphous powders, as resulting in the increasing magnitude of the K_I of 12.83 MPa (sample 1, 100 mm material height) and 19.29 MPa (sample 3) to 37.82 MPa (sample 2). Melting temperatures of the samples were determined by DSC. Results were directly corresponded to the cocoa butter content. The highest enthalpy of fusion (ΔH_m) of (23.32 ± 0.21) J/g was obtained for the highest cocoa butter containing sample 2 (of 20–22 wt. %). Obtained values of ΔH_m for samples 1 and 2 were of (12.38 ± 0.20) J/g and (10.27 ± 0.17) J/g. $T_{p\ (melt)}$ for reversing heat flow was ranging from (30.16 ± 0.10) °C to (32.28 ± 0.10) °C indicating the melting of stable β polymorph. The melting peaks observed at distinct temperatures in the non-reversing heat flow patterns were indicating melting of the unstable α and metastable β' and stable β cocoa butter polymorphic forms.

Introduction

The physical properties of powders, e.g., flowability, cohesion, adhesion, compression, etc., are influenced by the powders' composition. Measurement of the physical properties allows the understanding of powder behavior under the processing, packaging and storage conditions. The powder behavior is susceptible to change with the environment or surface and particles´ morphology. The powder behavior, as measured by acoustical performance testing and particle size distribution provides an insight into the surface behavior and the size of particles, which is an important factor influencing the physical properties of the dispersed system.[1] The variation in size, shape and properties of powders makes it difficult to establish the factors contributing to the powder rheology; however, it has been well reported that the chemical composition and

CONTACT Lubomír Lapčík ✉ lapcikl@seznam.cz Department of Physical Chemistry, Faculty of Science, The Palacky University Olomouc, 17. Listopadu 12, Olomouc 771 46, Czech Republic

surface properties of particles (including interactions and energetics) greatly influence its rheology.[2,3] The literature indicates an inverse relationship between the particle size and bulk density, consolidation behavior, and adhesivity between particles.[4] Stickiness in powders is a surface property occurring via five main mechanisms: intermolecular, electrostatic forces, mobile liquid bridges, solid bridges, and mechanical interlocking .[5,6] The interparticle interactions are also a characteristic of the particle's shape. The viscosity has been linked directly with the particle shape and inversely with the size and sphericity of the particle .[7] Food powders are of particular interest due to their increasing application in food and pharmaceutical manufacturing technologies.[8] The majority of food powders have fat particles incorporated in the microstructures of the bulk which gives them their characteristic flow property. However, like any other powders, the flowability of powders is essential in the industry to carry out many technological operations such as dosing, mixing, transport, packaging and hopper storage. Therefore, an extensive study of the mechanical properties of powders becomes essential. Our interest was focused on cocoa powders characterization due to their wide use in confectionery, baking and milk-based foods.

Cocoa (*Theobroma cocoa*) is originally a native of dense tropical forests in the Amazon. The first known cocoa plantations were established by the Maya in the lowlands of south Yucatan about 600 A.D. .[9] The genus *Theobroma* comprises more than 20 species, but only *T. cocoa* is of commercial importance. The seeds are fermented and processed to make cocoa butter (CB) and cocoa powder.[10] Further processing of CB and cocoa powder is prepared for the production of chocolates, confectioneries and beverages. The essential constituent of the cocoa powder is cocoa fat that determines the mechanical behavior of the product. Cocoa butter consists of triglycerols (95%), namely oleic acid (37%), stearic acid (32%), palmitic acid (27%), and linoleic acid (2–5) %.[11] The cocoa fat exhibits fascinating crystallization behavior that affects the sensorial and rheological properties of the cocoa products, especially chocolate. It exists in six different polymorphic crystalline states (I–VI) with distinguished melting temperatures.[12] The polymorphic states undergo transitions from one state to another depending on the processing temperature. The rheological properties of cocoa are primarily dependent on its composition and the presence of additives such as anticaking agents and emulsifiers.[13] Cocoa fat particularly the surface fat plays a vital role in providing structure to the cocoa powder, thereby influencing its utility. Commercial cocoa powders have the fat content ranging from 10 to 22 wt.%. Highly defatted cocoa powders contain less than 1 wt.% of the cocoa fat.[14] In the presented study, commercial cocoa powders with different cocoa fat contents were investigated. It is a well-known that cocoa powder is a versatile product and its functionality is defined by its composition. However, its composition depends on many parameters such as biological origin, pedological and agronomical conditions and raw material processing conditions.[15] Therefore, there was found in the literature, a relatively high compositional variability among the studied samples.[16,17] However, in this study, the composition information declared by the respective companies complies with European Union Regulation (EU) No. 1169/2011 (EFSA).[18]

There were studied mechanical and thermal properties to find out the relation between samples' fat contents and their collective mechanical properties, such as powder flowability and sound absorption performance. The latter parameters are affected by applied consolidation stresses during measurements influencing the packing density of the cocoa powder beds. Additionally, the thermal properties of the studied cocoa powders were determined by means of differential scanning calorimetry (DSC) and thermally modulated DSC (MDSC) method allowing in detail quantification of the melting heat flow patterns and crystalline cocoa butter polymorphic forms present in cocoa powder samples.

Materials and methods

Products

Three different commercial cocoa powders (see Tables 1 and 2) were tested in this study. The cocoa powders were kept in cool dry place at a constant laboratory temperature of 22°C and relative humidity of 35%.

Methodology

Particle size analysis

A vibratory sieve shaker Fritsch Analysette 3 (FRITSCH GmbH – Milling and Sizing, Idar-Oberstein, Germany), was used for the particle size analysis. The analysis was carried out three times using 150 g sample for each batch. Masses of individual fractions retained on the sieve screens were determined (applied sieves screen mesh diameters were as follows: 0.71, 0.56, 0.45, 0.32, 0.22, 0.16, 0.125, and 0.045 mm). The granulation of tested samples corresponded to granulation of fine flour (257 μm/96% to 162 μm/75%) and semi-coarse flour (366 μm/96% to 162 μm/75%). The mass average particle diameter (d_w) was calculated from the particle size distribution by the following formula[19]:

$$d_w = \frac{\sum (d_i \cdot w_i)}{\sum w_i} \tag{1}$$

where d_i is the average particle diameter of the individual fraction, and w_i is the weight fraction retained on the sieve. Samples were stored in the original package in dry form at ambient laboratory temperature of (25 ± 1) °C and relative humidity of 30%.

Differential scanning calorimetry thermal analysis

Thermal analysis was performed on a DSC 250 Discovery instrument (TA Instruments, New Castle, DE, USA) with T_{zero} measurement technology. The instrument was calibrated for indium standard (T_m = 156.6°C; ΔH = 28.45 J/g). Cocoa powder samples were weighed (5.0 ± 1.1) mg into aluminum pans and pressed with an aluminum lid. The measurement took place in an atmosphere of N_2 (50 ml/min flow rate); the heating rate was 10°C/min in the temperature range from 0 to 50°C. The melting temperature peak of cocoa butter was observed, and the results were expressed as T_{onset} (onset) and T_m (peak of melting temperature). Melting enthalpy ΔH_m was calculated by integrating the area under the thermograms and expressed as specific enthalpy in J/g (normalized enthalpy) at constant pressure.

Table 1. Sample description and labeling.

Sample labeling	d_w * (μm)	Cocoa fat concentration (w.%)	Bulk density (g/ml) Freely poured powder bed	Bulk density (g/ml) At 9 kPa consolidation stress	Sample description
1	238 ± 10	10	0.360	0.913	Cocoa powder Holland cocoa Dr. Oetker (Dr. Oetker, Ltd. Kladno, Czech Republic), acidity regulator (potassium carbonate).
2	125 ± 5	20–22	0.456	0.510	Cocoa powder (Kavoviny, JSC, Pardubice, Czech Republic), acidity regulator (potassium carbonate), soy lecithin.
3	303 ± 10	10–12	0.466	0.544	Cocoa powder Holland type Marila (Mokate Czech, Ltd., Prague, Czech Republic), acidity regulator (potassium carbonate).

*d_w _ mass average mean diameter.

Table 2. Composition of the studied cocoa powders.

Sample labeling	Energy (per 100 g) (kJ)	Fat (g) Total	Fat (g) Saturated	Carbohydrates (g) Total	Carbohydrates (g) Sugars	Proteins (g)	Salt (g)	Fibers (g)
1	1194	11	6.4	10	0.7	23	0.08	-
2	1460	13.7	7.5	17.1	0.6	24.6	1.98	24.6
3	1302	11	6.8	12.5	1	22	0.75	-

Temperature modulated differential scanning calorimetry

Temperature modulated differential scanning calorimetry (MDSC) was performed on a DSC 250 Discovery instrument (TA Instruments, New Castle, DE, USA) for resolution of polymorph type of cocoa butter in the samples. The instrument was calibrated for indium standard (T_m = 156.6°C; ΔH = 28.45 J/g). Cocoa powder samples were weighed (5 ± 0.1) mg into non-hermetic aluminum pans and sealed with an aluminum lid. An empty aluminum pan was used as a reference. The measurement was realized in an atmosphere of nitrogen (50 ml/min flow rate). The following temperature program was used: sample equilibration to 0°C by modulated temperature 1°C/120 s, isothermal crystallization at 0°C for 10 min, and subsequent heating to 50°C at a heating rate of 2°C/min. The temperature peaks related to cocoa butter melting were expressed as onset temperature $T_{o\ (melt)}$ and peak melting temperature $T_{p(melt)}$. Heat of fusion was calculated by integrating the area under the thermogram and expressed as melting enthalpy ΔH_{melt}. Reversing and non-reversing heat flows were used to split the endothermic melting peaks, representing heat capacity component (reversing curve) and kinetic component (non-reversing curve) .[20,21]

Gas chromatography-flame ionized detector (GC-FID)

Extraction of cocoa fat from cocoa powder samples was performed on Soxhlet extraction apparatus Soxtherm SOX 406 (Gerhardt GmbH & Co. KG, Wiesbaden, Germany) using n-hexane (97.0%, Chromasolv for GC, Sigma-Aldrich, St. Louis, USA) as extraction solvent. The extraction was applied for 2 h 22 min. Extracted fat fraction was concentrated by rotational vacuum evaporator Heidolph Hei-VAP equipped with a diaphragm pump Rotavac Vario Control (Heidolph Instruments GmbH & Co. KG., Schwabach, Germany). Samples of extracted cocoa butter were used for further analysis. Alkaline methyl-esterification of vacuum-dried samples was performed. The samples were mixed with 20 ml of 99.9% methanol (Honeywell, Charlotte, NC, USA). Then, 0.5 ml of 1 M methanolic potassium hydroxide solution and 0.5 ml of 99.0% toluene were added. Mixture was heated for 30 min under reflux. After cooling, 10 ml of 97.0% n-hexane and 20 ml of 20% brine were added and followed by a perfect shaking. Separated water layer was extracted with second volume of 10 ml n-hexane. Organic phases were mixed together, and afterward shaken with another 20 ml of brine. Total organic phase with standard Supelco 37 Component FAME Mix (Merck Millipore, Burlington, Massachusetts, USA) was dried applying sodium sulfate. Analysis of FAME samples was realized using Shimadzu GC-14A gas chromatography (GC) system (Shimadzu Corporation, Kyoto, Japan) with a flame ionization detector (FID). The separation was carried out on a DB-WAX capillary column (25 m length, 0.2 m internal diameter, 0.2 μm film thickness; Agilent Technologies, Santa Clara, CA, USA). Two microliters of sample were injected into a split mode (50:1) at a temperature of 225°C. Nitrogen was used as a carrier gas at constant flow rate of 2.82 ml/min. The programmed oven temperature was set as follows: 3 min at 110°C, 15°C/min up to 220°C, then held for 10 min. The detector temperature was 230°C. FAME sample identification was performed by direct comparison of their retention times with a purchased standard Supelco 37 Component FAME Mix (Supelco, Bellefonte, PE, USA). Three replicates were injected for each sample.

Acoustical performance measurements

The ability of granular powder materials to absorb sound is quantified by the sound absorption coefficient α, which is given by the ratio[22]:

$$\alpha = \frac{P_d}{P_i} \tag{2}$$

where P_d is the dissipated acoustic power in the tested material, and P_i is the incident acoustic power. The acoustic measurements were performed according to the ISO 10534–2 .[23,24] The normal incidence sound absorption coefficient α is defined:

$$\alpha = 1 - |r|^2 = 1 - r_r^2 - r_i^2 \tag{3}$$

where r is the normal incidence reflection factor, r_r and r_i are the real and imaginary parts of the normal incidence reflection factor. The noise reduction coefficient (NRC) takes into account the excitation frequency on the sound absorption coefficient. It is defined as the arithmetical average of the sound absorption coefficients of studied samples at the following excitation frequencies of 250, 500, 1000 and 2000 Hz[25,26]:

$$NRC = \frac{\alpha_{250} + \alpha_{500} + \alpha_{1000} + \alpha_{2000}}{4} \tag{4}$$

The speed of sound c of transmitting acoustic wave through powder beds is proportional to the primary absorption peak frequency f_{p1} as follows[27]:

$$c = 4 \cdot h \cdot f_{p1} \tag{5}$$

where h is the powder bed height. The longitudinal elastic coefficient K of the studied powder beds is equivalent with the Young's modulus of solid materials as follows[28]:

$$K = c^2 \cdot \rho_b = \left(4 \cdot h \cdot f_{p1}\right)^2 \cdot \rho_b \tag{6}$$

where ρ_b is the samples powder bed bulk density. Frequency dependencies of the normal incidence sound absorption coefficient were experimentally measured using a two-microphone impedance tube (BK 4206) in combination with a three-channel signal PULSE multi-analyzer (BK 3560-B-030) and power amplifier (BK 2706) in the frequency range of (200–6400) Hz (Brüel & Kjær, Nærum, Denmark). The normal incidence of sound absorption coefficient of freely poured samples with defined layer thickness (ranging from 15 to 100 mm) was determined. All experiments were performed under ambient laboratory conditions of 40% relative humidity and temperature of 22°C.

Scanning electron microscopy (SEM)

The SEM images were captured on Scanning Electron Microscope type Scios 2 Dual Beam (Thermo Fisher Scientific, Waltham, MA, USA) with accelerating voltage of 5 kV. For analyses, the samples were placed on a double-sided carbon tape on the aluminum holder and coated by 10 nm gold layer.

Statistical data analysis

Data were analyzed using a one-way analysis of variance (ANOVA method). Differences in the mean values among statistical groups were tested at a 0.05 significance level. Sigma Stat version 2.03 statistical software (Systat Software, Inc., San Jose, CA, USA) was used for data analysis. All experiments were performed on cocoa samples prepared in at least three replicates.

Results and discussion

Particle size and shape analysis

Captured SEM images of studied samples are shown in Figure 1. Here, a typical combination of crystal and amorphous regions can be distinguished. The studied cocoa powders exhibited a rounded shape of the individual cocoa particulates composed of mutually adhered cocoa fat micro/nano crystallites. Additionally, in the case of sample 3, there was found a spherical milk fat globule.[29] The highest cocoa fat crystal appearance was found for sample 1. The occurrence of ill-developed crystallites was the most profound in sample 2 similarly as found in the literature.[13,30] Mass average particle diameter (d_w) of (303 ± 10) μm was found for the sample 3, and the lowest one of (125.1 ± 5) μm was found for the sample 2. All results are summarized in Table 1 and Figure S1 (supplementary data).
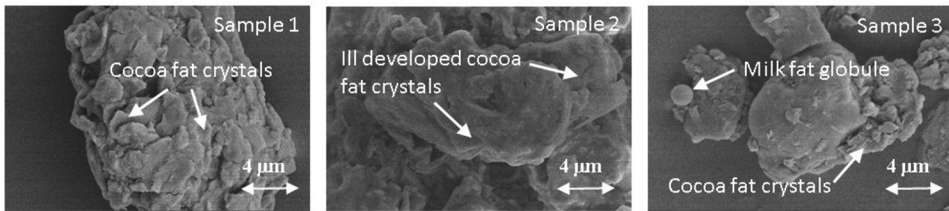
Figure 1. Comparison of mass average diameter of cocoa powders.

Differential scanning calorimetry thermal analysis

Results of the DSC thermal analysis of the studied cocoa powders are given in Table 3. Observed heating curves are depicted in Figure 2. There was found an excellent agreement between the declared cocoa fat content as presented by the manufacturers (Tables 1 and 2) and the values obtained on the basis of the measured melting heat of fusion. Melting enthalpy corresponded to the internal energy of the system, i.e. binding forces in the sample, and was related to the amount of cocoa powder triglycerides – oleic, palmitic and stearic acids. There were clearly distinguished the T_{onset} corresponding to the temperature at which the specific crystalline form begins to melt, the T_m corresponding to the maximum of the highest melting rate and the T_{end} corresponding to the end of heat of fusion peak completion, when all of the matter was being completely liquefied.[31] The T_{onset} fluctuated around the value of (26.14 ± 0.16) °C, and T_m of (31.65 ± 0.77) °C, regardless of the cocoa sample type.

Table 3. Results of the thermal analysis of the studied cocoa powders.

Sample	T_{onset}(°C)	T_m(°C)	T_{end}(°C)	ΔH_m(J/g)
1	26.29 ± 0.03	32.71 ± 0.07	36.54 ± 0.12	12.38 ± 0.20
2	25.92 ± 0.06	30.93 ± 0.10	34.15 ± 0.09	23.32 ± 0.21
3	26.22 ± 0.04	31.31 ± 0.08	35.13 ± 0.06	10.27 ± 0.17

Note: T_{onset} – onset melting temperature; T_m – peak melting temperature; T_{end} – end melting temperature; ΔH_m – melting enthalpy.
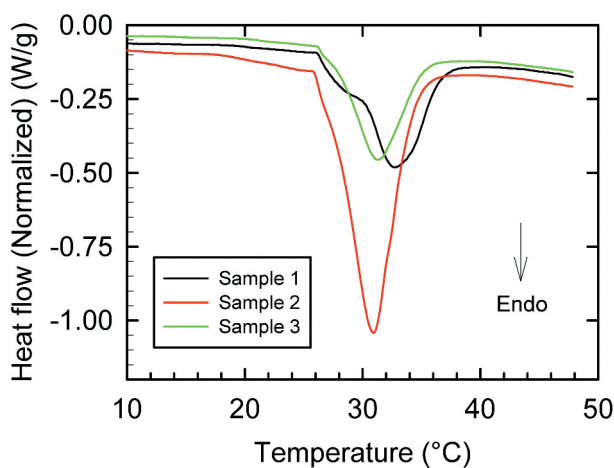

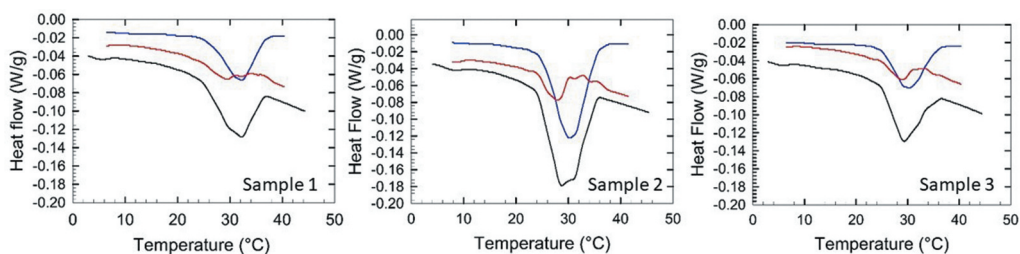Figure 2. Fusion enthalpy of cocoa butter for different cocoa powder samples.

Figure 3. Temperature modulated DSC thermograms of cocoa powder samples with detected endothermic peaks on total heat flow (black), reversing heat flow (blue) and non-reversing heat flow curves (red).

Temperature modulated differential scanning calorimetry (MDSC)

MDSC technique was used to characterize the melting profiles and the polymorphic forms of the cocoa butter in the tested samples (see Figure 3). The latter MDSC technique allows to separate total heat flow into two components (reversing and non-reversing). The reversing heat flow curve represents the process of molecular rearrangement (melting of fat crystals), whereas the non-reversing flow defines the kinetic events during the melting process. The sum of the reversing and non-reversing flows provides the total heat flow.[20] Using MDSC, complex thermal behavior of cocoa powder was observed, resulting from various crystal configurations of cocoa butter present in the samples.

From the total heat flow, there was found a higher peak melting temperature ($T_{p \text{ (melt)}}$) of (32.12 ± 0.09) °C for sample 1 in comparison to both the samples 2 and 3 where $T_{p \text{ (melt)}}$ was (28.71 ± 0.13) and (29.26 ± 0.15) °C, respectively. These were in an excellent corelation with the observed reversing melting peak temperature ($T_{p \text{ (melt)}}$) of (32.28 ± 0.1) °C compared to $T_{p \text{ (melt)}}$ of (30.16 ± 0.1) °C (sample 2) and (30.35 ± 0.14) °C (sample 3) (Table 4 and Fig. S2 in (Supplementary material)). These results were in association with the SEM analysis (Figure 1), for sample 1 which exhibited well-developed cocoa fat crystals.

Furthermore, in the measured non-reversing curves, there was observed a small peak in the temperature range of 22 to 23°C which was ascribed to the melting of unstable α modification of cocoa butter for all samples.[32–34] The observed melting peaks in the temperature range of 26 to 27°C were associated with the transition of unstable form III to metastable form IV (β' modification). Based on the available literature, it is worth mentioning that form III does not exist itself but it is a polymorph mixture of forms II (unstable α-modification) and form IV.[35–37] Observed peaks at the temperature of 28°C were attributed to the β' transition to (form IV) the stable β modification (form V).[38,39] Melting of β polymorph was observed in the temperature range of 29 to 34°C indicating a higher thermodynamic stability.[35] The results of our study correspond very well with melting peaks observed by[40] and crystalline polymorphic forms reviewed by[41] of cocoa butter with specific melting temperatures. The melting heat of fusion (ΔH_{melt}) of non-reversing heat flow represented minor values of total melting enthalpy, because cocoa powder samples adequately followed the temperature modulation in fashion typical for unstable crystallites that are not in thermodynamic equilibrium. The observed high value of ΔH_{melt} in the reversing heat flow curve was accredited to the crystallization of stable β polymorph which is typically appearing for stable crystals present in local equilibrium [42] (Table 4).

Gas chromatography-flame ionized detector (GC-FID)

Based on chromatographic peak area analysis, the main fatty acids present in cocoa powders were stearic acid C18:0 (32.15–33.70 wt.%), oleic acid C18:1 (31.75–32.25 wt.%) and palmitic acid C16:0 (27.60–28.60 wt.%), as given in Table 5. Each of the main fatty acids represented approximately one third of total fatty acid content. The observed quantities of major fatty acids were similar to those

Table 4. MDSC parameters of cocoa powder samples.

Sample	Heat flow			Reversing heat flow			Non-reversing heat flow		
	$T_{o\ (melt)}$(°C)	$T_{p\ (melt)}$(°C)	ΔH_{melt}(J/g)	$T_{o\ (melt)}$(°C)	$T_{p\ (melt)}$(°C)	ΔH_{melt}(J/g)	$T_{o\ (melt)}$(°C)	$T_{p\ (melt)}$(°C)	ΔH_{melt}(J/g)
1	25.08 ± 0.11	32.12 ± 0.09	11.05 ± 0.21	26.11 ± 0.14	32.28 ± 0.10	9.52 ± 0.08	25.09 ± 0.12	28.93 ± 0.13	0.93 ± 0.05
							31.27 ± 0.18	32.24 ± 0.08	0.10 ± 0.03
							34.33 ± 0.16	35.11 ± 0.10	0.02 ± 0.01
2	24.25 ± 0.10	28.71 ± 0.13	23.49 ± 0.24	25.28 ± 0.09	30.16 ± 0.10	21.36 ± 0.09	24.14 ± 0.17	27.70 ± 0.07	3.32 ± 0.06
							30.44 ± 0.12	31.15 ± 0.06	0.08 ± 0.02
							33.07 ± 0.18	34.04 ± 0.12	0.13 ± 0.04
3	24.65 ± 0.13	29.26 ± 0.15	10.57 ± 0.17	25.18 ± 0.10	30.35 ± 0.14	9.23 ± 0.10	25.10 ± 0.08	28.71 ± 0.14	1.60 ± 0.04
							31.31 ± 0.09	32.01 ± 0.11	0.001 ± 0.00
							33.95 ± 0.06	34.95 ± 0.07	0.07 ± 0.02

$T_{o\ (melt)}$ – onset melting temperature; $T_{p\ (melt)}$ – peak melting temperature; ΔH_{melt} – melting enthalpy. Results are stated as arithmetic mean ± standard deviation of three replicate measurements.

Table 5. Content of fatty acids (wt. %) in cocoa powders determined by GC-FID analysis.

Fatty acids	Sample 1	Sample 2	Sample 3
Palmitic acid C16:0	27.60 ± 0.10 [a]	28.10 ± 0.20 [b]	28.60 ± 0.20 [c]
Stearic acid C18:0	32.15 ± 0.35 [a]	33.70 ± 0.10 [b]	32.50 ± 0.50 [a]
Oleic acid C18:1	31.90 ± 0.40 [a]	32.25 ± 0.15 [a]	31.75 ± 0.35 [a]
Lauric acid C12:0	1.05 ± 0.05 [a]	0.50 ± 0.00 [b]	0.85 ± 0.05 [c]
Myristic acid C14:0	2.60 ± 0.00 [a]	1.40 ± 0.00 [b]	2.30 ± 0.10 [c]
Myristoleic acid C14:1	0.30 ± 0.00 [a]	n. d.	0.10 ± 0.05 [b]
Palmitoleic acid C16:1	0.50 ± 0.00 [a]	0.50 ± 0.20 [a]	0.20 ± 0.10 [a]
Margaric acid C17:0	0.70 ± 0.30 [a]	0.25 ± 0.05 [b]	0.15 ± 0.05 [b]
α-Linoleic acid C18:2	2.45 ± 0.05 [a]	2.40 ± 0.10 [a]	2.60 ± 0.20 [a]
Arachidic acid C20:0	0.85 ± 0.15 [a]	0.90 ± 0.10 [a]	0.95 ± 0.05 [a]

n. d. – not detected. Results are stated as arithmetic mean ± standard deviation of three replicates. The values followed by the same letters in the same raw are not significantly different at significance level α ≤ 0.05 by Tukey test.

found by other authors.[40,43,44] Minor amounts of the other fatty acids determined were unsaturated linoleic acid C18:2 (2.40–2.60 wt.%), saturated myristic acid C14:0 (1.40–2.60 wt.%), lauric acid C12:0 (0.50–1.05 wt.%) and arachidic acid C20:0 (0.85–0.95 wt.%). Fatty acids determined in low quantities was myristoleic acid (C14:1) (present in low-fat samples 1 and 3 in traces (≤0.30 wt.%)). However, it was not detected in sample 2 of high fat content. The fatty acid content statistically varied between the samples (Tukey test, α ≤ 0.05) for palmitic and stearic acid, although there was no variation in the oleic acid content for all three samples.

Acoustical performance measurements

Material's sound absorption is governed by several factors such as excitation frequency, material thickness, porosity and density.[45] Frequency dependencies of the sound absorption coefficient are shown in Figures 4 and 5. As clear from Figure 4, the lowest sound absorption was found for sample 2 indicating its higher compact structure compared to samples 1 and 3. Interestingly, both lower fats containing cocoa samples 1 and 3 exhibited occurrence of the sound absorption peak maximum at the primary absorption peak frequency f_{p1} of 440 Hz. The decreasing cocoa powders' particle size led to the increasing contact area available, thus increasing adhesive forces. This might have resulted in higher structural compactness. The latter increase of the sound absorption of the lower fat content cocoa powders as reflected in the higher magnitudes of the observed NRC indicates a strong effect of cocoa fat crystallite platelet edges on interparticle packing loose structure with increased nano/micro sized voids. It can be assumed that the latter crystalline morphology occurrence in samples 1 and 3 might be due to the absence of the fiber content unlike sample 2, where more amorphous structure of the badly developed cocoa fat structures was observed due to the declared fiber content of 24.6 w.% (Table 2) which is expected to be detrimental for adequate cocoa fat crystal formation.[46] Mechanical
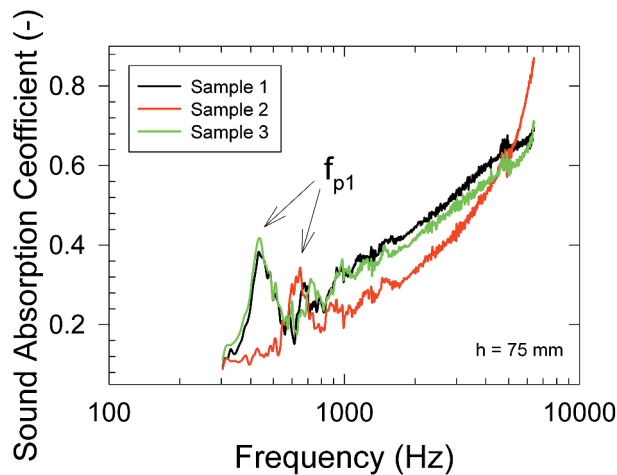
Figure 4. Frequency dependencies of the sound absorption coefficient of the studied cocoa powders as obtained for 75 mm powder bed height.
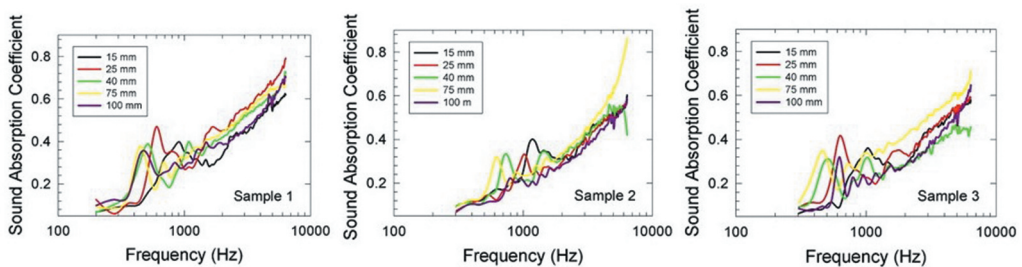

Figure 5. Results of the frequency dependency patterns of the sound absorption coefficient of the tested cocoa powders bed height.

stiffness of the powders was investigated based on the speed of sound (c) and the longitudinal modulus of elasticity from equations 5 and 6. There was found the highest magnitude of the longitudinal modulus of elasticity (K_l) of 37.8 MPa for the 100 mm powder bed of the sample 2 indicating the compact character of the powder bed compared to samples 1 and 3 (12.8 MPa and 19.3 MPa) where more porous structures were observed. With the increasing powder bed height (up to 75 mm), the primary absorption peak frequency was shifted to lower frequencies as shown in Figure 4, which was reflected in the higher mechanical stiffness (K_l) of the studied cocoa powders (Table 6). At the highest powder bed height of 100 mm, the primary absorption peak frequency was shifted to higher frequencies.

Powder rheology

Results of the powder rheological measurements are summarized in Table 7 and Figure 6. Flowable materials at the zero normal stress exhibited zero value of the shear stress, hence resulting in the yield stress curve crossing the intercept at the origin. As evident from Figure 6(a) obtained yield locus dependencies were typical for cohesive powders, as the intercepts of the observed flow patterns were the highest for samples 1 and 3 (1.68 kPa and 1.76 kPa). Observed cohesion value of 0.75 kPa for sample 2 indicated a better flowability in comparison with the samples 1 and 3. These results were in agreement with the flow factor (FF) values, where for sample 2 the flow factor was of 5.46 indicating cohesive character of the powder; however, the values of FF for samples 1 and 3 were in the range of

Table 6. Results of the sound absorption measurements of the studied loose powder beds.

Sample	Quantity	Material height [mm]				
		15	25	40	75	100
1	NRC [–]	0.229	0.259	0.321	0.281	0.289
	f_{p1} [Hz]	928	600	504	432	472
	c [m·s^{-1}]	55.7	60.0	80.6	129.6	188.8
	K_I [MPa]	1.12	1.30	2.34	6.05	12.83
2	NRC [–]	0.203	0.208	0.191	0.191	0.182
	f_{p1} [Hz]	1168	1016	736	648	720
	c [m·s^{-1}]	70.1	101.6	117.8	194.4	288.0
	K_I [MPa]	2.24	4.71	6.32	17.23	37.82
3	NRC [–]	0.202	0.201	0.287	0.282	0.227
	f_{p1} [Hz]	1048	600	504	440	512
	c [m·s^{-1}]	62.9	60.0	80.6	132.0	204.8
	K_I [MPa]	1.82	1.66	2.99	8.12	19.29

Table 7. Results of the powder rheology measurements.

Sample	Consolidation stress (kPa)	Cohesion (kPa)	FF (–)	AIF (°)	UYS (kPa)	MPS (kPa)	MCS (kPa)
1	9	1.68	2.67	30.35	5.85	15.64	3.22
2	3	0.25	5.86	27.72	0.82	4.80	1.45
2	6	0.26	10.22	31.14	0.92	9.41	2.70
2	9	0.75	5.46	30.95	2.66	14.53	3.81
2	15	1.35	5.12	28.41	4.52	23.16	6.62
3	9	1.76	2.39	33.72	6.58	15.74	2.62

Abbreviations: FF – flow factor, AIF – angle of internal friction, UYS – unconfined yield strength, MPS – major principal stress, MCS – minor consolidation stress.
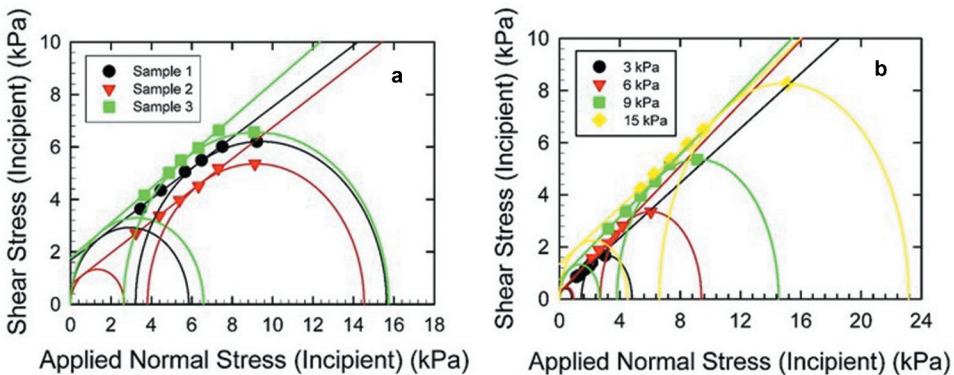
Figure 6. Yield locus of the studied cocoa powders (a) at 9 kPa consolidation stress, (b) flow curves obtained for the sample 2 at varying consolidation stresses as mentioned in the legend.

2.39 to 2.67 typical for highly cohesive powders. There was confirmed the increasing trend of the cohesion with the increasing consolidation stress as shown in Figure 6(b) indicating the rising cohesiveness of the powders.

Conclusion

It was found in this study that the cocoa powders´ yield loci patterns were of cohesive to highly cohesive character as indicated by increased factor from 2.39 (sample 1) and 2.67 (sample 3) typical for highly cohesive powders and to 5.46 for sample 2 typical for cohesive powders. It was clearly demonstrated that the cocoa powders of higher crystalline structure (samples 1 and 3) were less flowable compared to the

ones with the more amorphous character (sample 2) as indicated by decreased cohesion from 1.68 kPa and 1.76 kPa to 0.75 kPa. It was confirmed by SEM analysis that the studied cocoa powders of higher cocoa fat and dietary fiber contents were more amorphous in nature. It was proposed that the dietary fibers hindered the creation of the well-developed crystals. Observed low sound absorption patterns indicated relatively dense packing of the high cocoa fat powder sample 2 typical for non-porous materials. The latter observations were supported by the observed increase of the structural mechanical stiffness as represented by K_I of the freely poured powder bed of the high cocoa fat amorphous powder (sample 2) in comparison to samples 1 and 3 from 37.82 MPa (material height of 100 mm) to 12.83 MPa and 19.29 MPa respectively. MDSC demonstrated cocoa butter polymorph transition, detected by reversing and non-reversing heat flow curves. Cocoa powder samples adequately followed the applied temperature modulation resulting in minor values of total melting enthalpy (on non-reversing heat flow curves) typical for unstable polymorphs. Transition of metastable β' cocoa butter crystalline modification was detected around the melting point of 28°C; melting of stable β polymorph was found in temperature range of 29 to 34°C. Resulting thermal parameters of cocoa powders correlated with fatty acids content determined by GC-FID analysis. The main fatty acids determined were stearic acid C18:0 (32.15–33.70 wt.%), oleic acid C18:1 (31.75–32.25 wt.%) and palmitic acid C16:0 (27.60–28.60 wt.%). Statistically significant differences were found for palmitic and stearic acid contents as evaluated by Tukey test, α ≤ 0.05.

Disclosure statement

No potential conflict of interest was reported by the author(s).

Funding

ORCID

Lubomír Lapčík ⬤ http://orcid.org/0000-0002-9917-7310
Barbora Lapčíkova ⬤ http://orcid.org/0000-0002-4713-0502
Shweta Gautam ⬤ http://orcid.org/0000-0003-1545-2205
Martin Vašina ⬤ http://orcid.org/0000-0002-8506-098X
Tomáš Valenta ⬤ http://orcid.org/0000-0001-5683-5718
David Řepka ⬤ http://orcid.org/0000-0002-8340-6246
Klára Čépe ⬤ http://orcid.org/0000-0003-4962-2399
Ondřej Rudolf ⬤ http://orcid.org/0000-0002-5549-9385

References

[1] Figura, L.; Teixeira, A. A. *Food Physics: Physical properties-measurement and Applications*; Springer Science & Business Media: Berlin, 2007; pp 73–115.

[2] Cuq, B.; Rondet, E.; Abecassis, J. Food Powders Engineering, between Knowhow and Science: Constraints, Stakes and Opportunities. *Powder Technol.* 2011, *208*(2), 244–251. DOI: 10.1016/j.powtec.2010.08.012.

[3] Montes, B. C.; Martínez-Alejo, J. M.; Lozano-Perez, H.; Gumy, J. C.; Zemlyanov, D.; Carvajal, M. T. A Surface Characterization Platform Approach to Study Flowability of Food Powders. *Powder Technol.* 2019, *357*, 269–280. DOI: 10.1016/j.powtec.2019.08.072.

[4] Ahmed, J.; Al-Foudari, M.; Al-Salman, F.; Almusallam, A. S. Effect of Particle Size and Temperature on Rheological, Thermal, and Structural Properties of Pumpkin Flour Dispersion. *J. Food Eng.* 2014, *124*, 43–53. DOI: 10.1016/j.jfoodeng.2013.09.030.

[5] Boonyai, P.; Bhandari, B.; Howes, T. Stickiness Measurement Techniques for Food Powders: A Review. *Powder Technol.* 2004, *145*(1), 34–46. DOI: 10.1016/j.powtec.2004.04.039.

[6] Jacquot, C.; Petit, J.; Michaux, F.; Montes, E. C.; Dupas, J.; Girard, V.; Gianfrancesco, A.; Scher, J.; Gaiani, C. Cocoa Powder Surface Composition during Aging: A Focus on Fat. *Powder Technol.* 2016a, *292*, 195–202. DOI: 10.1016/j.powtec.2016.01.032.

[7] Ben Trad, M. A.; Demers, V.; Dufresne, L. Effect of Powder Shape and Size on Rheological, Thermal, and Segregation Properties of low-pressure Powder Injection Molding Feedstocks. *J. Mater. Eng. Perform.* 2019, *28*(9), 5551–5562. DOI: 10.1007/s11665-019-04276-9.

[8] Lapčík, L.; Otyepka, M.; Otyepková, E.; Lapčíková, B.; Gabriel, R.; Gavenda, A.; Prudilová, B. Surface Heterogeneity: Information from Inverse Gas Chromatography and Application to Model Pharmaceutical Substances. *Curr. Opin. Colloid Interface Sci.* 2016, *24*, 64–71. DOI: 10.1016/j.cocis.2016.06.010.

[9] Lapčík, L.; Lapčíková, B.; Žižková, H.; Li, P.; Vojteková, V. Effect of Cocoa Fat Content on Wetting and Surface Energy of Chocolate. *Potravinarstvo Slovak J Food Sci.* 2017, *11*(1), 410–416. DOI: 10.5219/732.

[10] Minifie, B. *Chocolate, Cocoa and Confectionery: Science and Technology*; Springer Science & Business Media, 2012; pp 3–34.

[11] Afoakwa, E. O. *Cocoa Production and Processing Technology*; CRC Press, 2014.

[12] Palmieri, P. A.; Hartel, R. W. Crystallization of Cocoa Butter in Cocoa Powder. *J. Am. Oil Chem. Soc.* 2019, *96*(8), 911–926. DOI: 10.1002/aocs.12247.

[13] Lapčíková, B.; Lapčík, L.; Salek, R.; Valenta, T.; Lorencová, E.; Vašina, M. Physical Characterization of the Milk Chocolate Using Whey Powder. *LWT.* 2022, *154*, 112669. DOI: 10.1016/j.lwt.2021.112669.

[14] Do, T.; Vieira, J.; Hargreaves, J. M.; Mitchell, J. R.; Wolf, B. Structural Characteristics of Cocoa Particles and Their Effect on the Viscosity of Reduced Fat Chocolate. *LWT Food Sci. Technol.* 2011, *44*(4), 1207–1211. DOI: 10.1016/j.lwt.2010.10.006.

[15] Foubert, I.; Vanrolleghem, P. A.; Thas, O.; Dewettinck, K. Influence of Chemical Composition on the Isothermal Cocoa Butter Crystallization. *J. Food Sci.* 2004, *69*(9), E478–E487. DOI: 10.1111/j.1365-2621.2004.tb09933.x.

[16] Adeyeye, E. I.; Tripathi, S. Proximate, Mineral and Antinutrient Compositions of Natural Cocoa Cake, Cocoa Liquor and Alkalized Cocoa Powders Sourced in Nigeria. *J. Adv. Pharmaceutical Sci.Technol.* 2016, *1*(3), 12–28. DOI: 10.14302/.2328-0182.japst-15-855.

[17] Ilori, O. A.; Olorode, O. O.; Albert, O. M. Physical Characteristic, Proximate Composition, Polyphenol and Antinutritional Factors of Chocolate Produced from New Nigerian Cocoa Variety. *Int. J. Novel Res. Interdisci. Stud.* 2021, *8*, 4.

[18] European Parliament. Mandatory Food Information, 2022 Aug 18.

[19] Svensson, D. N.; Messing, I.; Barron, J. An Investigation in Laser Diffraction Soil Particle Size Distribution Analysis to Obtain Compatible Results with Sieve and Pipette Method. *Soil Tillage Res.* 2022, *223*, 105450. DOI: 10.1016/j.still.2022.105450.

[20] Leyva-Porras, C.; Cruz-Alcantar, P.; Espinosa-Solís, V.; Martínez-Guerra, E.; Piñón-Balderrama, C. I.; Compean Martínez, I.; Saavedra-Leos, M. Z. Application of Differential Scanning Calorimetry (DSC) and Modulated Differential Scanning Calorimetry (MDSC) in Food and Drug Industries. *Polymers.* 2019, *12*(1), 5. DOI: 10.3390/polym12010005.

[21] Tolstorebrov, I.; Eikevik, T. M.; Bantle, M. A DSC Determination of Phase Transitions and Liquid Fraction in Fish Oils and Mixtures of Triacylglycerides. *Food Res. Int.* 2014, *58*, 132–140. DOI: 10.1016/j.foodres.2014.01.064.

[22] Sgard, F.; Castel, F.; Atalla, N. Use of a Hybrid Adaptive Finite element/modal Approach to Assess the Sound Absorption of Porous Materials with meso-heterogeneities. *Appl. Acoustics.* 2011, *72*(4), 157–168. DOI: 10.1016/j.apacoust.2010.10.011.

[23] Han, F.; Seiffert, G.; Zhao, Y.; Gibbs, B. Acoustic Absorption Behaviour of an open-celled Aluminium Foam. *J. Phys. D: Appl. Phys.* 2003, *36*(3), 294. DOI: 10.1088/0022-3727/36/3/312.

[24] ISO, I. 10534-2: Acoustics-Determination of Sound Absorption Coefficient and Impedance in Impedance tubes-Part 2: Transfer-function Method. *BS EN ISO.* 2001, 10534–10532.

[25] Buratti, C. Indoor Noise Reduction Index with an Open Window (Part II). *Appl. Acoustics.* 2006, *67*(5), 383–401. DOI: 10.1016/j.apacoust.2005.07.006.

[26] Tiwari, V.; Shukla, A.; Bose, A. Acoustic Properties of Cenosphere Reinforced Cement and Asphalt Concrete. *Appl. Acoustics.* 2004, *65*(3), 263–275. DOI: 10.1016/j.apacoust.2003.09.002.

[27] Okudaira, Y.; Kurihara, Y.; Ando, H.; Satoh, M.; Miyanami, K. Sound Absorption Measurements for Evaluating Dynamic Physical Properties of a Powder Bed. *Powder Technol.* 1993, *77*(1), 39–48. DOI: 10.1016/0032-5910(93)85005-T.

[28] Yanagida, T.; Matchett, A. J.; Coulthard, J. M.; Asmar, B. N.; Langston, P. A.; Walters, J. K. Dynamic Measurement for the Stiffness of Loosely Packed Powder Beds. *AIChE J.* 2002, *48*(11), 2510–2517. DOI: 10.1002/aic.690481110.

[29] Lapčík, L.; Lapčíková, B.; Otyepková, E.; Otyepka, M.; Vlček, J.; Buňka, F.; Salek, R. N. Surface Energy Analysis (SEA) and Rheology of Powder Milk Dairy Products. *Food Chem.* 2015, *174*, 25–30. DOI: 10.1016/j.foodchem.2014.11.017.

[30] Afoakwa, E. O.; Paterson, A.; Fowler, M.; Vieira, J. Characterization of Melting Properties in Dark Chocolates from Varying Particle Size Distribution and Composition Using Differential Scanning Calorimetry. *Food Res. Int.* 2008a, *41*(7), 751–757. DOI: 10.1016/j.foodres.2008.05.009.

[31] Afoakwa, E. O.; Paterson, A.; Fowler, M.; Vieira, J. Characterization of Melting Properties in Dark Chocolates from Varying Particle Size Distribution and Composition Using Differential Scanning Calorimetry. *Food Res. Int.* 2008b, *41*(7), 751–757. 10.1016/j.foodres.2008.05.009.

[32] Deora, N. S.; Misra, N. N.; Deswal, A.; Mishra, H. N.; Cullen, P. J.; Tiwari, B. K. Ultrasound for Improved Crystallisation in Food Processing. *Food Eng. Rev.* 2013a, *5*(1), 36–44. DOI: 10.1007/s12393-012-9061-0.

[33] Pore, M.; Seah, H. H.; Glover, J.; Holmes, D. J.; Johns, M. L.; Wilson, D. I.; Moggridge, G. D. In-situ X-ray Studies of Cocoa Butter Droplets Undergoing Simulated Spray Freezing. *J. Am. Oil Chem. Soc.* 2009, *86*(3), 215–225. DOI: 10.1007/s11746-009-1349-8.

[34] Smith, K. W.;. Cocoa Butter and Cocoa Butter Equivalents. In *Structured and Modified Lipids*, 2001; pp 401–422.

[35] Afoakwa, E. O.; Paterson, A.; Fowler, M. Factors Influencing Rheological and Textural Qualities in chocolate–a Review. *Trends Food Sci. Technol.* 2007, *18*(6), 290–298. DOI: 10.1016/j.tifs.2007.02.002.

[36] Deora, N. S.; Misra, N. N.; Deswal, A.; Mishra, H. N.; Cullen, P. J.; Tiwari, B. K. Ultrasound for Improved Crystallisation in Food Processing. *Food Eng. Rev.* 2013b, *5*(1), 36–44. 10.1007/s12393-012-9061-0.

[37] Ribeiro, A. P. B.; Masuchi, M. H.; Miyasaki, E. K.; Domingues, M. A. F.; Stroppa, V. L. Z.; de Oliveira, G. M.; Kieckbusch, T. G. Crystallization Modifiers in Lipid Systems. *J. Food Sci. Technol.* 2015, *52*(7), 3925–3946. DOI: 10.1007/s13197-014-1587-0.

[38] Joshi, B. L.; Zielbauer, B. I.; Vilgis, T. A. Comparative Study on Mixing Behavior of Binary Mixtures of Cocoa butter/tristearin (CB/TS) and Cocoa butter/coconut Oil (CB/CO). *Foods*. 2020, *9*(3), 327. DOI: 10.3390/foods9030327.

[39] Talhat, A. M.; Lister, V. Y.; Moggridge, G. D.; Rasburn, J. R.; Wilson, D. I. Development of a Single Droplet Freezing Apparatus for Studying Crystallisation in Cocoa Butter Droplets. *J. Food Eng.* 2015, *156*, 67–83. DOI: 10.1016/j.jfoodeng.2015.02.010.

[40] Jacquot, C.; Petit, J.; Michaux, F.; Montes, E. C.; Dupas, J.; Girard, V.; Gianfrancesco, A.; Scher, J.; Gaiani, C. Cocoa Powder Surface Composition during Aging: A Focus on Fat. *Powder Technol.* 2016b, *292*, 195–202. 10.1016/j.powtec.2016.01.032

[41] Ghazani, S. M.; Marangoni, A. G. Molecular Origins of Polymorphism in Cocoa Butter. *Ann. Rev. Food Sci. Technol.* 2021, *12*(1), 567–590. DOI: 10.1146/annurev-food-070620-022551.

[42] Toledo, M.;. Analysis of Melting Process Using TOPEM ®. In *Mettler Toledo Thermal Analysis UserCom 25, Mettler-Toledo AG*. 2010.

[43] ElKhori, S.; Paré, J. J.; Bélanger, J. M.; Pérez, E. The microwave-assisted Process (MAPTM1): Extraction and Determination of Fat from Cocoa Powder and Cocoa Nibs. *J. Food Eng.* 2007, *79*(3), 1110–1114. DOI: 10.1016/j.jfoodeng.2006.01.089.

[44] Ramos-Escudero, F.; Casimiro-Gonzales, S.; Á, F.-P.; Chávez, K. C.; Gómez-Mendoza, J.; de la Fuente-Carmelino, L.; Muñoz, A. M. Colour, Fatty Acids, Bioactive Compounds, and Total Antioxidant Capacity in Commercial Cocoa Beans (Theobroma Cacao L.). *LWT*. 2021, *147*, 111629. DOI: 10.1016/j.lwt.2021.111629.

[45] Lapčík, L.; Vašina, M.; Lapčíková, B.; Otyepková, E.; Waters, K. E. Investigation of Advanced Mica Powder Nanocomposite Filler Materials: Surface Energy Analysis, Powder Rheology and Sound Absorption Performance. *Compos. B Eng.* 2015, *77*, 304–310. DOI: 10.1016/j.compositesb.2015.03.056.

[46] Lapčíková, B.; Burešová, I.; Lapčík, L.; Dabash, V.; Valenta, T. Impact of Particle Size on Wheat Dough and Bread Characteristics. *Food Chem.* 2019, *297*, 124938. DOI: 10.1016/j.foodchem.2019.06.005.